RESEARCH ARTICLE

Nitrogen pollution and sources in an aquatic system at an agricultural coastal area of Eastern China based on a dual-isotope approach

Yanqiang Li[1,2] · Weijin Yan[1] · Fang Wang[1] · Shucong Lv[1,2] · Qingqian Li[1,2] · Qibiao Yu[1,2]

Abstract

Nitrogen (N) pollution of water courses is a major concern in most coastal watersheds in eastern China with intensive agricultural production. We use hydrogeological and dual-isotopic approaches to analyze the N concentrations, pollution, transformations, and sources of surface water and groundwater in an agricultural watershed of the Jiaozhou Bay (JZB) area. Results showed that dissolved total N (DTN) concentrations in sub-rivers (SRs) ranged from 6.0 to 25.3 mg N L^{-1} in the dry season and 9.1–26.7 mg N L^{-1} in the wet season, which indicated a positive relationship with the percentages of agricultural land. Meanwhile, the dominant dissolved N species in SRs changed from nitrate (NO_3^-, 64–100%) to dissolved organic N (DON, 52–77%) from the dry season to the wet season and the increased DON concentrations showed a positive relationship with the planted proportions of vegetable production systems. The NO_3^- concentrations of groundwaters ranged from 10.6 to 121.4 mg N L^{-1}, which were over the limit for drinking water by the World Health Organization. Isotopic analysis indicated that most NO_3^- originated from the microbiological conversion via nitrification, whereas the deletion of denitrification was insignificant in this area. The results of the stable isotope analysis in R mixing model showed the contributions of potential NO_3^- sources which were in order of manure fertilizers (20.6–69.0%) > soil organic matter (19.5–53.2%) > chemical fertilizers (5.5–34.3%) > atmospheric deposition (1.3–18.8%). This study suggests that the management of crop productions and reasonable manure fertilizer application should be implemented to protect the quality of aquatic systems in the JZB area.

Keywords Nitrogen pollution · Dual isotopes · Cropping systems · Intensive agricultural activities · Aquatic systems · Jiaozhou Bay

Introduction

The loading of reactive nitrogen (N) to aquatic systems, such as surface rivers and groundwaters, has increased significantly in the coastal watersheds of Eastern China through the influence of anthropogenic activity (Wang et al. 2015; Yu et al. 2015). For instance, the dissolved inorganic nitrogen (DIN) losses from lands to Changjiang River increased from 22 to 445 kg N km^{-2} $year^{-1}$ during 1970 to 2003 (Wang et al. 2015). Consequently, not only are aquatic systems in watersheds polluted by the increasing reactive N, but fluvial transport and submarine groundwater discharge (SGD) also increase the quantity of N exported to the coastal bays/estuaries deteriorating the water quality of freshwater and seawater in coastal areas (Zhang 2007; Liu et al. 2012; Jin et al. 2013; Yu et al. 2015; Yuan et al. 2016). Coastal areas occupy only 13% of the national land area, but provide 60% of the gross domestic product, largely through agriculture. The high density of human activities in these areas can, therefore, strongly influence N loading on aquatic systems, particularly in agricultural dominant watersheds where fertilizer is increasingly applied to enhanced crop productions. While some studies have demonstrated that agroecosystems are the largest sources of N to aquatic systems

✉ Weijin Yan
   yanwj@igsnrr.ac.cn

[1] Institute of Geographic Sciences and Natural Resources Research, Chinese Academy of Sciences, Beijing 100101, China

[2] University of the Chinese Academy of Sciences, Beijing 100049, China

(Howarth 2008; Han et al. 2014), the influences of associated agricultural activities on N pollution in aquatic systems in coastal areas are far from being understood.

Nitrogen losses from soil to water aquatic systems have a positive relationship with excess N in a watershed (Yan et al. 2010; Liu et al. 2012; Yu et al. 2015). Anthropogenic activities, predominantly intensive agriculture, are the main cause of increased excess N across regional, national, and global scales (Howarth 2008; Yan et al. 2010; Han et al. 2014). Han et al. (2014) showed that net anthropogenic nitrogen inputs increased from 2360 to 5013 kg N km^{-2} $year^{-1}$ from 1981 to 2009, due to the fertilizer application increasing from 1000 to 3040 kg N km^{-2} $year^{-1}$. Studies modeling the riverine nitrogen exported from watersheds in Eastern China have also demonstrated that the fluvial N transport is closely associated with fertilizer application in coastal areas (Yan et al. 2010; Yu et al. 2015). In agricultural practices, the amount and species of fertilizer used is tailored to the requirements of specific crops (Babiker et al. 2004; Russo et al. 2017; Winings et al. 2017). For example, the amount of fertilizer applied to vegetable production systems (VPS) is notably higher than that applied to grain production systems (GPS) (Zhao et al. 2014; Shen et al. 2017; Zhang et al. 2017). While manure fertilizer (MF) is typically used in VPS, chemical fertilizer (CF) is often used in GPS (Zhang et al. 2017). Driven by the requirement for rising income, considerable areas of GPS were gradually replaced by VPS in many coastal regions of china in recent decades (Lv 2011; Li 2014). For example, the cultivated area of grains decreased from 80 to 69% and the cultivated area of vegetables increased from 2 to 12% between 1980 and 2009 in coastal areas (Li 2014). Thus, analyzing the N pollution in response to agricultural activities can improve the understanding of N loading to surface rivers, groundwaters, and coastal bays/estuaries under the enhanced human activities.

Among the multiple N species, nitrate (NO_3^-) contamination is a pervasive problem in most agricultural areas in the world (Babiker et al. 2004; Zhang et al. 2014; Ji et al. 2017). A number of studies have demonstrated that NO_3^- is the primary cause of environment problems, such as water eutrophication, toxic algal blooms, reducing biodiversity, and health problems (Zhang 2007; Liu et al. 2012; Jin et al. 2013; Yu et al. 2015; Yuan et al. 2016). High concentrations of NO_3^- in drinking water also present a risk to human health, having been linked to an increased risk of cancer and infectious diseases (Mckenzie and Townsend 2007). The NO_3^- concentrations of surface water and groundwater are influenced by multiple factors, including the mixing of different sources and biological processes (Xue et al. 2009). In recent years, studies have successfully assessed the NO_3^- pollution by identifying the NO_3^- potential sources and determining the NO_3^- transformation based on the isotopic approach (Xue et al. 2009; Ji et al. 2017; Parnell et al. 2013; Crawford et al. 2017). The δ^{15}N-NO_3^- and δ^{18}O-NO_3^- of different sources have certain

specific value ranges due to the processes occurring during the synthesis of NO_3^- (Xue et al. 2009; Choi et al. 2017; Crawford et al. 2017). CF (such as ammonium fertilizer, NO_3^- fertilizer, and urea) shows typical values between -6 to $+6‰$ (Jr and Bonner 2010); the δ^{15}N-NO_3^- values from atmospheric deposition (AD) range between -13 and $+13‰$ (Heaton 1986; Kendall 1998); the δ^{15}N values of NO_3^- originating from MF vary between $+4$ to $+25‰$; the typical δ^{15}N values of soil organic N (SN) range from 0 to $+8‰$ (Xue et al. 2009). The O-NO_3^- of AD originates from O_2 (δ^{18}O = 23.5‰) which resulted in a large variability of δ^{18}O-NO_3^- from $+25$ to $+75‰$ (Kendall 1998; Xue et al. 2009) as well as the δ^{18}O in fertilizer NO_3^- (Amberger and Schmidt 1987; Oelmann et al. 2007). The δ^{18}O-NO_3^- from MF and SN is related to other sources with lower values between -5 and $+10‰$ (Xue et al. 2009). The combination of the δ^{15}N and δ^{18}O-NO_3^- values provides unique information of NO_3^- origins in aquatic systems. Nitrification and denitrification are two primary biological process of N recycle, which transforms NH_4^+ into NO_3^- and dissolved NO_3^- to N_2 or N_2O (Well and Flessa 2009; Yin et al. 2017; Crawford et al. 2017). However, the origins of sources in watershed N enrichment are not changeless among various watersheds, due to mixing of different N sources and spatial variability in inputs and transformations across variable hydrologic conditions (Xue et al. 2009; Ji et al. 2017; Parnell et al. 2013; Xing and Liu 2016). For example, Xing and Liu (2016) found no obvious signs of denitrification to delete the NO_3^- concentrations of surface rivers in Loess Plateau of China; the study of Ji et al. (2017) demonstrated the significant denitrification of groundwater in the agricultural watershed of Changle River in Zhejiang Province; and Ding et al. (2015) found minor nitrification in the surface river of an agricultural watershed in Taihu Lake Basin. Based on isotopic compositions of NO_3^-, four potential NO_3^- sources have been quantified by a Bayesian isotope mixing model (stable isotope analysis in R (SIAR) mixing model); the results were also various in different regions (Parnell et al. 2013; Ding et al. 2015; Korth et al. 2014; Xing and Liu 2016). Therefore, clarifying the influences of potential factors on the concentration, environmental behavior and potential sources of NO_3^- will advance the knowledge on enhanced human activities on potential N pollution in freshwater and coastal bays/estuaries.

Jiaozhou Bay (JZB), located southeast of Shandong Peninsula, is an example of a typical semi-closed bay of China (China Soil Database). The dissolved inorganic N concentrations and nutritional condition index in JZB have increased from 0.1 to 0.5 mg N L^{-1} and from ~0.3 to 4.2, respectively, in recent years. These increases frequently cause toxic algae blooms in summer (Yuan et al. 2016). There is evidence that the increasing total nitrogen (TN) of sediments in JZB is associated with anthropogenic activities (Kang et al. 2017). The Dagu River (DGR) watershed is the largest

agricultural watershed in the JZB area. In this study, we delineated the watershed into 11 sub-watsheds according to the sub-rivers. We collected water samples from surface water and groundwater based on the sub-watersheds in both the dry and wet seasons. The study aims were to measure the dissolved N concentrations and species in surface water and groundwater and analyze the N pollution in response to influencing factors, determine the isotopic signatures of NO_3^- and H_2O ($\delta^{15}N$ and $\delta^{18}O$) in surface water and ground water to identify the potential sources of NO_3^-, clarify NO_3^- transformations, and quantify the contributions of potential NO_3^- sources in aquatic systems.

Methods and material

Studying site

The DGR watershed (119° 46′ 58″–120° 37′ 40″ E, 35° 54′ 10″–37° 23′ 42″ N) is located in the Jiaozhou Bay region, Shandong Province, East China (Fig. 1). The watershed is in the temperate continental monsoon climate zone with distinctive dry and wet seasons. The average annual temperature is 12.2 °C, with the minimum of − 12 °C in January and maximum of 38 °C in August. The annual rainfall volume varies from 462.1 to 909.2 mm, with 70–80% of the total precipitation occurring from June to September (Yellow River Hydrologic Year Book 1999–2008). The DGR, as the longest river with an average discharge of ∼ 1.88×10^8 m^3 $year^{-1}$ into the JZB, accounts for 85% of the water flux from the JZB to the Yellow Sea (Yellow River Hydrologic Year Book 1999–2008). Via the tool of ArcGIS, we extract the DGR watershed from the Digital Elevation Model (DEM, 30×30 m) and delineate the watershed into 11 sub-watsheds. Based the sub-rivers, the sub-watsheds were named Zhu River (ZR) watershed, Xiaogu River (XGR) watershed, Wugu River (WGR) watershed, Changguang River (CGR) watershed, Chengzi River (CZR) watershed, Luoyao River (LYR) watershed, Liuhao River (LHR) watershed, Taoyuan River (TYR) watershed, Nanjiaolai River (NJLR) watershed, and Yunxi River (YXR) watershed (Fig. 1). In the source region of DGR, there are many small sub-rivers and we put them together as one sub-watershed, which is named Junwu River (JWR) watershed (Fig. 1). The catchment area of DGR covers 6045 km^2, of which 74% is used for agriculture, 13% for residential land, 8% for grassland, 3% for the waterbody, and 2% for forest. In sub-watsheds, the agricultural land ranged from to 58 to 92%, which are also dominated types of land use in each sub-watershed. Details about the land uses of sub-watsheds are provided in Table 1. In the watershed, the GPS are maize and wheat. As the requirement for high economic benefit, the GPS has been replaced by the VPS (including carrot, potato, onion, ginger, and Chinese onion) in recent

decades. The spatial distributions of rotation compositions were various in sub-watsheds with 38–60% of VPS and 40–62% of GPS (Table 1, the data of different crop production systems were collected from Qingdao Agricultural Technology Extension Station).

For the sampling sites, we selected the sub-river mouth as the sampling sites of SRs. In the JWR watershed, we selected the JWR as the sampling river to represent the sub-rivers in the source region. For SGW sampling sites, we selected the nine sites within 1 km of the relative sites of SRs in sub-watsheds. We did not select the SGW and SR samples in the YXR sub-watershed because of the aquatic systems influenced by the JZB. Also, we did not collect the SGW sample in the CGR watershed because of no wells were found in the sub-watershed. In DGR, we selected ten sites (1–10) based on the river mouths of sub-rivers. The details of sampling sites are shown in Fig. 1.

Water samples

Sampling was conducted in December 2016 and October 2017, representing the dry and wet seasons, respectively. At each sampling site, the pH, temperature (°C), and dissolved oxygen (DO) concentrations were measured in situ using a portable meter (YSI 550A). All sampling equipment was pre-cleaned with deionized water. River samples at the 20-cm depth in the middle of the river were collected by PM–polyethylene on the bridge near the mouth of SRs. Groundwater samples at 30-cm depth were collected by pre-cleaned polyethylene from the private dug wells installed into 6–10 m depth from the ground surface by farmers in their agricultural fields. In each sampling site, 250 mL water was filtered through 0.45-μm membrane filters on the sampling day and saved into pre-cleaned polyethylene bottles. The filtrate was divided 50 ml for stable isotope analysis and 200 ml for the nitrogen analysis, and stored in a freezer (− 4 °C) before analysis.

Analytical methods

Nitrogen analysis

The N analysis includes nitrate (NO_3^-), nitrite (NO_2^-), ammonium (NH_4^+), dissolved inorganic nitrogen (DIN), dissolved organic nitrogen (DON), and dissolved total nitrogen (DTN) (Table 2 and 3). All analysis was carried out on the filtered water samples (Sect. 2.2). The NO_3^-, NH_4^+, and NO_2^- concentrations were measured using ultraviolet spectrophotometry (Goldman and Jacobs 1961), Nessler's reagent colorimetric method (GB 7479-87 1987), and the Griess–Saltzman method (Trivelin et al. 2002), respectively. The DTN was digested using alkaline potassium persulfate at 120–124 °C for 30 min and then analyzed spectrophotometrically at
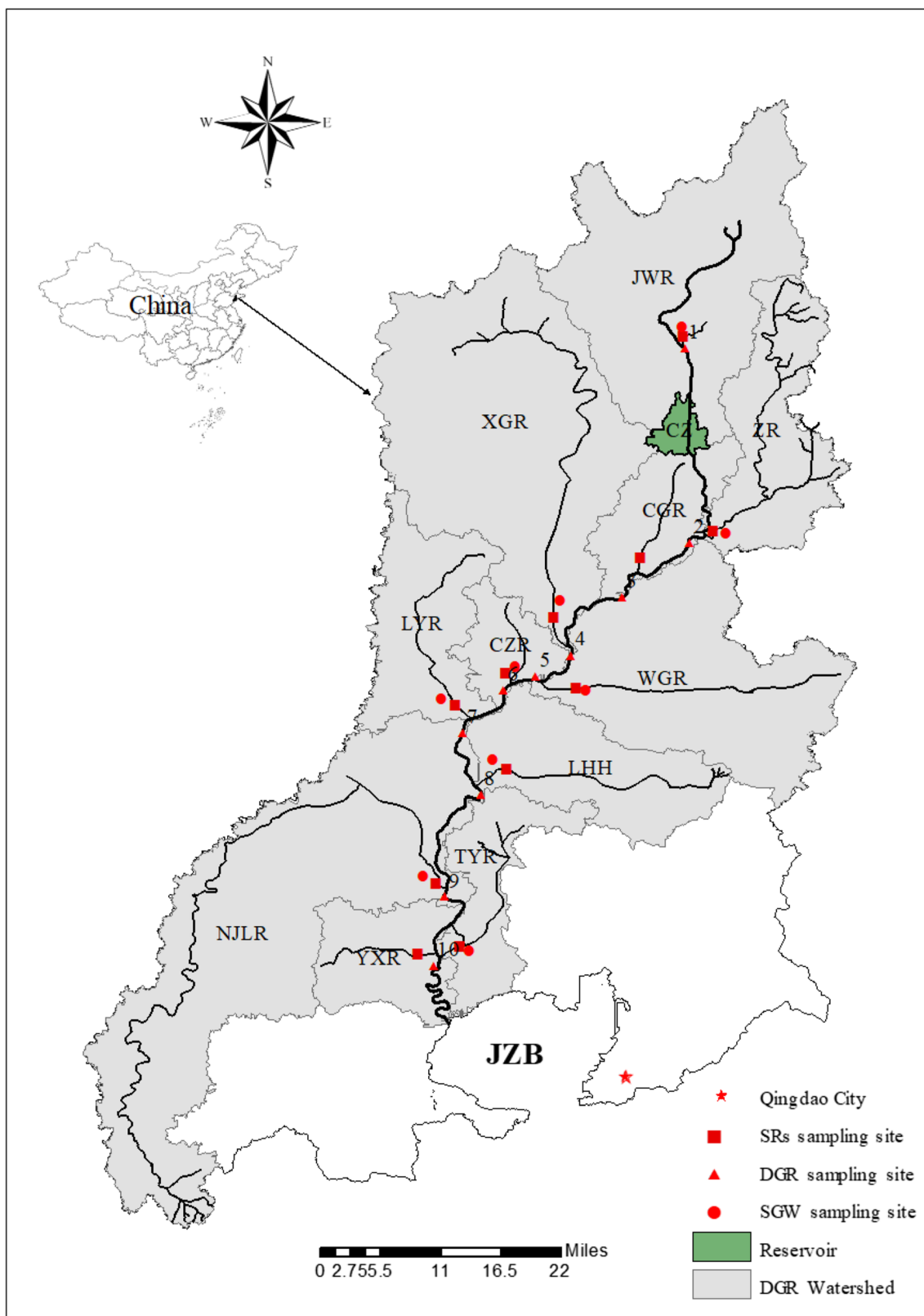
Fig. 1 Location of the Dagu River watershed and the sampling sites. Square denotes the sampling site of the surface river, triangle denotes the sampling site of Dagu River, and circle denotes the sampling site of groundwater. Abbreviations; JZB: Jiaozhou Bay; JWR: Junwu River; XGR: Xiaogu River; ZR: Zhu River; WGR: Wugu River; LHR: Liuhao River; NJLR: Nanjiaolai River; TYR: Taoyuan River; CZR: Chengzi River; CGR: Changguang River; YXR: Yunxi River; CZ: Chanzhi Reservoir; DGR: Dagu River; SRs: sub-rivers of Dagu River; SGW: groundwater in sub-watersheds

Table 1 Land use compositions and c ropping systems compositions of sub-watersheds in Dagu River watershed in 2016

Sub-watersheds	Area ×10⁴ hm²	Agricultural land %	VPS	GPS
JWR	8.5	72.2	38	62
ZHR	3.9	72.6	50	50
CGR	2.1	91.1	50	50
XGR	11.0	71.5	59	41
WGR	7.2	88.3	51	49
CZR	1.3	85.0	52	48
LYR	3.5	81.8	55	45
LHR	3.8	85.9	60	40
NJLR	13.1	77.7	51	49
TYR	2.4	68.8	40	60
YXR	2.4	46.4	56	44
DGR	61.3	73.4	51	49

Data of land uses originated from National Earth System Science Data Sharing Infrastructure n.d. (http://www.geodata.cn/), and the data of cropping systems originated from Qingdao Agricultural Technology Extension Station

JWR Junwu River, *ZR* Zhu River, *CGR* Changguang River, *XGR* Xiaogu River, *WGR* Wugu River, *LYR* Luoyao River, *LHR* Liuhao River, *NJLR* Nanjiaolai River, *TYR* Taoyuan River, *CZR* Chengzi River, *YXR* Yunxi River, *VPS* vegetable production system, *GPS* grain production system

275 nm and 220 nm (D'Elia and Steudler 1977). The DIN concentrations are the sum of the NO_3^-, NH_4^+, and NO_2^- concentrations; the DON concentrations were calculated based on the difference between DTN and DIN.

Isotope compositions of water and nitrate

$\delta^{15}N/\delta^{18}O\text{-}NO_3^-$ In this study, we used the bacterial denitrification method to determine $\delta^{15}N/\delta^{18}O\text{-}NO_3^-$ (Sigman et al. 2001). This method simultaneously provides results on $\delta^{15}N$ and $\delta^{18}O$ based on the conversion of NO_3^- and N_2O using denitrifying bacteria (Xue et al. 2009). First, the strains are cultivated. The denitrifying bacterial cultures are cultivated for 6–10 days in amended tryptic soy broth (TSB) to obtain the magnitude of the biomass. Second, the concentration of bacterial clusters is determined. After the cultivation, the TSB substrates are divided into 40mL centrifuge tubes and centrifuged. The supernatant of the centrifugation is then decanted and reserved and the tubes with the sediments are pipetted using 4 mL fresh TSB to determine the concentrations (10-fold) of denitrifying bacteria. Third, an anaerobic environment is created. The tubes with concentrated substrates are homogenized and transferred into 20mL headspace vials. To keep the anaerobic conditions and remove the prior N_2O, the vials are purged with N_2 gas for 3 h before they are crimp-sealed with Teflon-backed silicone septa. Fourth,

the samples are cultivated. A total of 20 mL of each sample is injected into the headspace vials and incubated for 24 h to ensure the complete conversion of NO_3^- to N_2O. Fifth, measurements are carried out. After cultivation of the samples, the headspace vials are injected into 0.1 mL 10 N NaOH to stop the bacterial activity. Subsequently, N_2O is extracted to measure the $\delta^{15}N$ and $\delta^{18}O$ via isotope ratio mass spectrometry.

The nitrogen and oxygen isotopic ratios (R) are reported based on the millesimal (mil) deviation from the $^{15}N/^{14}N$ or $^{18}O/^{16}O$ ratios relative to N_2 (air) and Standard Mean Ocean Water (SMOW), respectively. The $\delta^{15}N\text{-}NO_3^-$ and $\delta^{18}O\text{-}NO_3^-$ values are defined as

$$\delta\,(\%) = \frac{R_{\text{sample}} - R_{\text{standard}}}{R} \times 1000 \qquad (1)$$

$\delta^{18}O$ of H_2O The isotopic compositions of oxygen ($\delta^{18}O\text{-}H_2O$) of all water samples were analyzed with a Micromass IsoPrime mass spectrometer coupled to an automated line based on the equilibration between $O\text{-}H_2O$ and CO_2 gas. The $\delta^{18}O\text{-}H_2O$ values have a precision of 0.2‰.

Quantification of the contributions of nitrate sources

Based on the Bayesian framework, Parnell and Jackson (2008) developed a stable isotope analysis in R (SIAR) model to establish a logical prior distribution using the Dirichlet distribution to estimate the possible proportional source contribution and determine the probability distribution for the proportional contribution of each source to the mixture (http://cran.R-project.org/web/packages/siar/index.html). By defining a set of N mixture measurements and j ($\delta^{15}N$ and $\delta^{18}O\text{-}NO_3^-$) isotopes with k source contributors, the mixing model can be expressed as follows (Xue et al. 2009):

$$X_{ij} = \sum_{k=1}^{k} p_k \times (s_{jk} + c_{jk}) + \varepsilon_{jk} \qquad (2)$$

$$s_{jk} \sim N(\mu_{jk}, \omega^2)$$

$$\varepsilon_{ij} \sim N(0, \sigma^2{}_j)$$

$$c_{jk} \sim N(\lambda_{jk}, \tau^2{}_{jk})$$

where X_{ij} is the isotope value j of the mixture i with $i = 1,2, 3,\ldots, N$ and $j = 1, 2, 3,\ldots, J$; s_{jk} is the source value k of the isotope j ($k = 1, 2, 3,\ldots, k$) and is normally distributed with a mean μ_{jk} and standard deviation ω_{jk}; p_k is the proportion of source k, which needs to be estimated with the SIAR model; c_{jk} is the fractionation factor for isotope j of source k and is normally distributed with a mean λ_{jk} and standard deviation τ_{jk}; and ε_{ij} is the residual error representing the additional unquantified variation between individual mixtures and is normally distributed with a mean 0 and standard deviation σ_j.

Table 2 The physicochemical and isotopic values of aquatic systems in the dry season

Sample		pH	T °C	DO (mg L⁻¹)	N-NO₃⁻ mg N L⁻¹	N-NH₄⁺	N-NO₂⁻	DIN	DON	TDN	δ^{15}N-NO₃⁻ ‰	δ^{18}O-NO₃⁻	δ^{18}O-H₂O
SRs	JWR	8.3	7.4	7.0	12.6	1.0	0.1	13.7	2.6	16.3	8.7	5.3	− 10.2
	CGR	7.2	6.9	5.0	17.8	2.7	0.0	20.5	1.7	22.2	14.4	5.9	− 9.9
	ZR	7.9	5.8	5.8	11.0	0.3	0.0	11.2	3.0	14.2	8.5	8.1	− 9.5
	XGR	7.9	7.9	6.8	12.9	0.7	0.0	13.6	3.7	17.3	11.5	3.5	− 9.8
	CZR	7.7	7.0	10.0	15.5	0.8	0.0	16.3	8.4	24.8	11.6	4.8	− 9.9
	WGR	8.4	8.2	5.0	20.5	0.6	0.1	21.1	4.2	25.3	13.0	1.1	− 9.9
	LYR	8.4	4.8	4.0	15.6	0.5	0.0	16.1	3.3	19.4	6.7	1.9	− 10.0
	LHR	8.4	6.6	3.0	16.2	0.5	0.0	16.7	6.3	23.0	2.6	6.2	− 9.7
	NJLR	8.3	6.9	3.0	11.0	0.5	0.0	11.5	3.5	15.0	9.5	− 1.2	− 9.6
	TYR	8.6	5.8	7.0	5.6	0.1	0.0	5.7	0.3	6.0	10.5	− 5.3	− 9.3
DGR	1	8.6	5.8	5.2	7.8	0.1	0.1	7.9	0.3	8.3	10.5	− 5.3	− 9.3
	2	8.3	5.9	7.0	12.6	1.0	0.0	13.6	1.6	15.2	8.7	5.3	− 9.0
	3	7.9	6.8	3.8	13.8	0.1	0.0	13.9	0.1	14.0	9.7	3.5	− 9.7
	4	8.6	5.7	4.3	10.3	0.5	0.0	10.8	1.1	11.9	0.3	15.7	− 10.4
	5	8.4	5.4	3.8	13.8	0.5	0.0	14.3	1.4	15.7	14.6	3.7	− 10.0
	6	8.3	6.5	6.8	9.8	1.0	0.0	10.7	0.3	11.0	9.8	1.9	− 10.0
	7	7.4	3.9	4.0	8.0	0.1	0.0	8.1	2.2	10.3	11.5	0.7	−10.0
	8	9.0	6.8	3.8	11.8	1.0	0.0	12.7	1.3	14.0	9.8	1.9	−9.5
	9	8.4	7.7	4.7	10.3	0.2	0.0	10.5	2.3	12.8	2.3	16.5	− 10.0
	10	8.7	0.0	5.2	8.9	1.1	0.1	10	1.1	11.1	9.8	9.8	− 10.0
SGW	JWR watershed	6.5	15.2	1.6	27.7	0.3	0.2	28.0	1.2	29.2	7.3	1.2	− 9.7
	ZR watershed	6.0	15.9	1.7	32.0	0.7	0.1	32.7	5.3	38.0	13.2	2.6	− 9.5
	XGR watershed	7.1	14.9	3.5	48.2	0.2	0.1	48.4	5.8	54.2	11.3	3.1	− 9.7
	CZR watershed	5.3	15.4	0.3	78.7	0	0.1	78.7	1.5	80.3	6.0	2.1	− 9.1
	WGR watershed	7.2	16.5	5.1	54.5	0.4	0.0	54.9	0.9	55.8	11.7	− 0.6	− 9.0
	LYR watershed	5.3	14.2	3.5	61.1	0.1	0.0	61.2	4.2	65.4	4.9	− 0.9	− 10.2
	LHR watershed	6.4	15.2	4.2	97.7	1.7	0.0	59.3	2.6	65.5	3.3	10.9	− 9.7
	NJLR watershed	6.2	15.7	3.5	25.7	0.3	0.0	26.0	0.4	26.4	6.8	7.1	− 10
	TYR watershed	7.2	16.2	0.5	76.9	0.8	0.1	77.8	0.9	78.6	15.7	4.2	− 9.0

JWR Junwu River, *ZR* Zhu River, *CGR* Changguang River, *XGR* Xiaogu River, *WGR* Wugu River, *LYR* Luoyao River, *LHR* Liuhao River, *NJLR* Nanjiaolai River, *TYR* Taoyuan River, *CZR* Chengzi River, *SRs* are sub-rivers, *SGW* is groundwater in sub-watersheds

Results and discussion

Characteristics and spatial patterns of N distribution

N concentrations in surface water and groundwater

The DTN concentrations of surface water and groundwater had a wide range between different sub-watersheds. In SRs, the DTN concentrations ranged from 6.0 to 25.3 mg N L⁻¹ in the dry season and 9.1–26.7 mg N L⁻¹ in the wet season (Table 2 and 3). Values were typically higher in SGW, ranging from 26.4 to 80.3 mg N L⁻¹ in the dry season and 10.9 to 122.5 mg N L⁻¹ in the wet season. WGR and TYR had the largest and smallest DTN concentrations in both the wet and dry seasons, respectively. Land use has been demonstrated as a primary factor influencing the loss of N from soil to flow into rivers or leach into groundwater (Filoso et al. 2003; Wolters et al. 2016; Xing and Liu 2016). Among the various land covers, the agricultural lands suffered the largest N losses to aquatic systems. Yaşar Korkanç and Dorum (2019) showed that the N losses from fields covered by crops were significantly higher than the abandoned farmland, plantation areas, and rangelands under similar rainfall conditions. In this study, the DTN concentrations of SRs showed a positive relationship with the percentages of agricultural land in the sub-watersheds (Fig. 2a). In the wet season, a similar relationship was also found between the N concentrations of SGW and the percentages of agricultural lands in sub-watersheds, except in XGR (Fig. 2b). This indicates that agricultural lands are the primary sources contributing DTN to surface rivers and groundwater in the DGR watersheds.
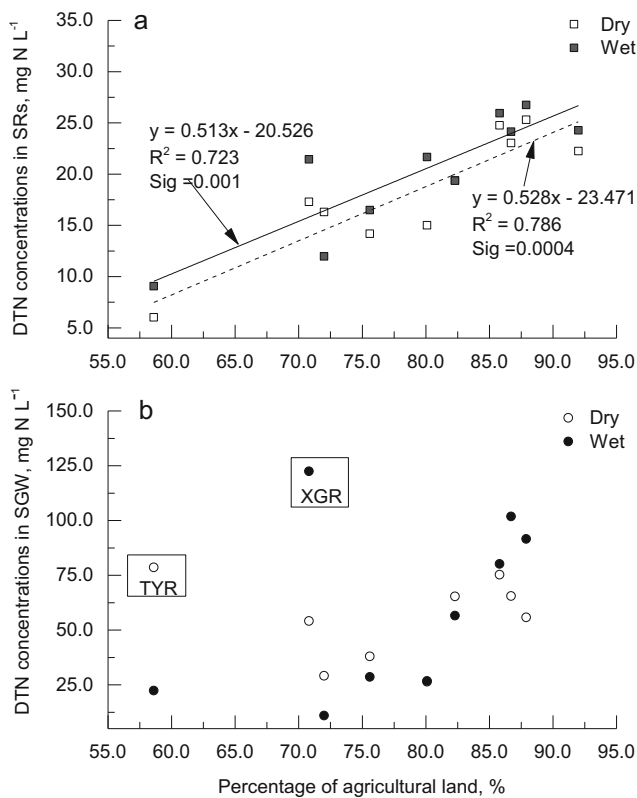
Fig. 2 Relationship between DTN concentrations in **a** sub-rivers and **b** groundwater and percentage of agricultural lands in sub-watersheds. Solid line denotes linear fit in the wet season and dashed line denotes linear fit in the dry season. Abbreviations: DGR: Dagu River; SRs: sub-rivers of Dagu River; SGW: groundwater in sub-watersheds

Fig. 3 Relationship between DTN concentrations in **a** sub-rivers and **b** groundwater and compositions of crop rotations in sub-watersheds. Solid line denotes linear fit in the wet season and dashed line denotes linear fit in the dry season. Abbreviations: MEC: modern economic crop rotation; SRs: sub-rivers of Dagu River; SGW: groundwater in sub-watersheds

In agricultural lands, growing crops have been demonstrated as a primary factor that impact nutrient loss via surface runoff (García-Díaz et al. 2017; Yaşar Korkanç and Dorum 2019; Yi et al. 2018). Previous studies have shown that N losses due to surface runoff and leaching were positively correlated with the amount of fertilizer applied (Zhao et al. 2014; Chen et al. 2017). The amount of N fertilization applied to production of grains was 160–240 kg N hm^{-2} (Ju et al. 2009; Zhang et al. 2017), and the value was 300–3816 kg N hm^{-2} for production of vegetables (Kou et al. 2005; Shen et al. 2017). The DTN runoff loss from fields grown with vegetables (5.9–15.5 kg N hm^{-2} $year^{-1}$) was higher than that from the fields grown with maize (0.8 kg N hm^{-2} $year^{-1}$) (Wang et al. 2019; Yi et al. 2018). In this study, the DTN concentrations of surface water and groundwater showed positive with the planted proportions of VPS in the wet season (Fig. 3). Therefore, VPS are likely to be responsible for the increasing dissolved N loads of aquatic systems in the wet season.

N compositions of surface water and groundwater

Studies found that the dominant N species is DIN in surface waters in agricultural watersheds (Jin et al. 2015;
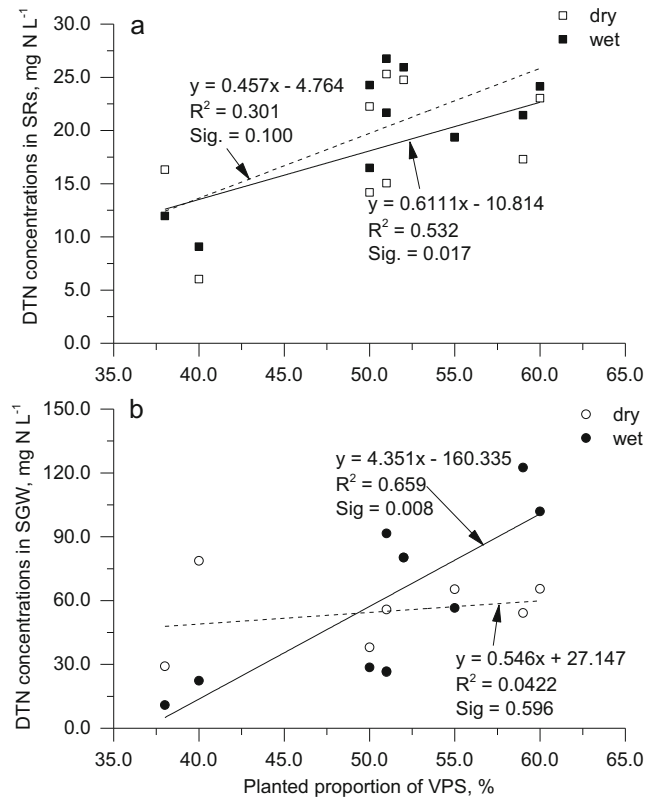
Ding et al. 2015) and DON in surface rivers located in areas with low levels of human activity (Xing and Liu 2016). In this study, NO_3^- and DON were the two primary N species across the coastal watershed. However, the compositions of N species in surface rivers showed distinctive seasonal changes (Fig. 4). NO_3^- was the dominant N species in the SRs (64–100%) in the dry season, whereas DON (52–77%) was dominant in the wet season (Fig. 4a). The NO_3^- concentrations of SRs ranged from 5.8 to 20.5 mg N L^{-1} in the dry season. During the dry season, with the exception of TYR, the NO_3^- concentrations in 90% of sub-rivers were higher than the limit of 10 mg N L^{-1} for drinking water set by the World Health Organization (WHO). In comparison, during the wet season the values of NO_3^- concentrations of SRs decreased to 2.6–6.9 mg N L^{-1}, which are lower than the WHO standard for drinking water. The decreasing NO_3^- concentrations of surface rivers during the wet season is attributable to dilution effects from increased precipitation (Ding et al. 2015) or transformation by enhanced denitrification (Jr and Bonner 2010). The JZB area is located in the temperate continental monsoon climate zone, with 70–80% of the total precipitation occurring during the wet season (June to September). However, the denitrification
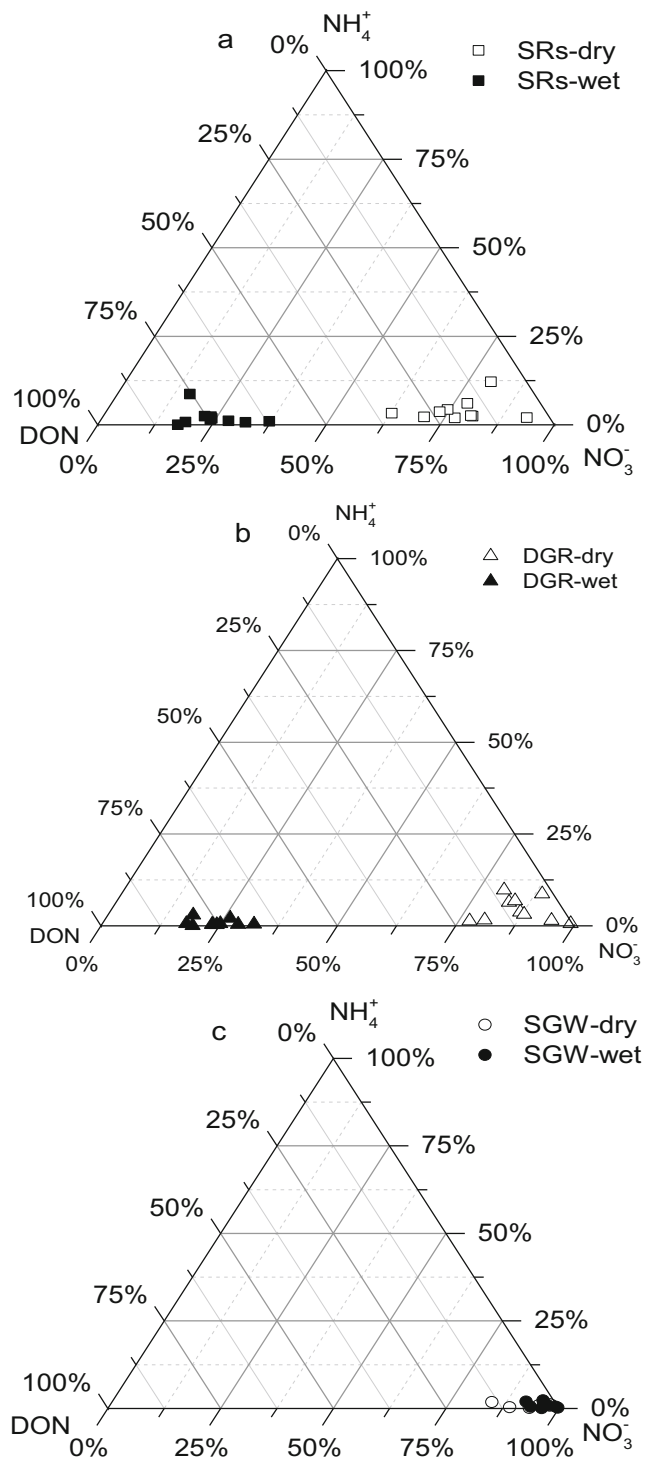
Fig. 4 Compositions of N forms in aquatic systems in Dagu River watershed: **a** is the compositions of N forms in sub-rivers, **b** is the compositions of N forms in Dagu River, and **c** is the compositions of N forms in groundwater. Abbreviations: DGR: Dagu River; SRs: the sub-rivers of Dagu River; SGW: groundwater in sub-watersheds

was insignificant in SRs as discussed below (Sect. 3.2.2). Therefore, the decreasing NO_3^- concentrations due to enhanced precipitation in this study area.

Unlike seasonal changes of NO_3^- concentrations, DON concentrations of SRs increased from 0.3–8.4 mg N L^{-1} in the dry season to 2.6–19.9 mg N L^{-1} in the wet season and the percentage of DON increased from 0 to 34% in the dry season to 52–77% in the wet season (Fig. 4a). This indicates that the increased external DON loses to SRs due to the enhanced precipitation during the wet season. Human activities influence the DON loss by wastewater discharges (Xing and Liu 2016). In this study, TYR is characterized by the largest density of human population and the lowest agricultural activity, whereas the DON concentration of the TYR in the wet season was lower than that of other sub-rivers with higher agricultural lands in their catchments (Table 3). This indicated that the DON in surface river originated from agricultural productions, indirectly.

Fertilizer application has demonstrated the largest N sources in agricultural dominated regions (Howarth 2008; Han et al. 2014). Dissolved N losses from the agricultural lands closely associated with the fertilizer application due to surface runoff. CF (ammonia fertilizer, urea, and nitrate fertilizer) is often used in the production of grains, whereas the production of vegetables is usually associated with large amounts of MF (including cow and horse, pig, and sheep and poultry) (Zhang et al. 2017). The VPR occupied 38–60% of arable areas in sub-watersheds (Table 1). The enhanced cultivation of vegetables is expected to lead to an increase in the application of MF to agricultural lands, which will increase the organic N in surface soil. Studies have shown that DON loss via surface runoff is higher from fields grown vegetables (4.2–7.2 kg N hm^{-2} $year^{-1}$) than that from fields grown with cereal (0.8–3.2 kg N $h\,m^{-2}$ $year^{-1}$) (Yi et al., 2018; Manninen et al. 2018). In SRs, the percentages of DON in DTD showed a positive relationship with the cultivated proportions of VPS in the wet season (Fig. 5). According to the field investigation by our team, the DON concentrations in surface water from fields grown with vegetables (DON 15.1–18.4 mg N L^{-1}) were obviously higher than that in surface water from fields grown with grains (DON 2.3–2.8 mg N L^{-1}). Thus, the increasing DON concentration of SRs in the wet season is strongly attributable to the cultivation of vegetables in the sub-watersheds.

The dominant N species of SGW was NO_3^- in both the dry and wet seasons, which occupied 86–99% and 93–99% of TN, respectively (Fig. 4c). The high percentages of NO_3^- in groundwater are often attributed to the freedom of NO_3^- transport via leaching, compared with other N species (Meybeck 1982; Zhang et al. 2014; Xing and Liu 2016). In this study, the NO_3^- concentrations were 25.7–78.7 mg N L^{-1} in the dry season and the values were 10.6–121.4 mg N L^{-1} in the wet season (Table 2 and 3). It should be noticed that the NO_3^- concentrations in all SGW samples were over the limit of 10 mg N L^{-1} for the drinking water set by the WHO. It should be noted that the NO_3^- concentration of SGW is higher than

Table 3 The physicochemical and isotopic values of aquatic systems in wet season

Sample		pH	T °C	DO (mg L^{-1})	N-NO$_3^-$ mg N L^{-1}	N-NH$_4^+$	N-NO$_2^-$	DIN	DON	TDN	δ^{15}N-NO$_3^-$ ‰	δ^{18}O-NO$_3^-$	δ^{18}O-H$_2$O
SRs	JWR	8.6	26.1	5.6	3.8	0.1	0.0	3.9	8.1	12.0	9.7	3.5	− 9.0
	CZR	7.7	28.2	6.5	5.4	0.6	0.0	6.0	18.3	24.3	13.6	3.2	− 9.9
	ZR	7.7	26.7	4.3	2.6	1.4	0.0	4.0	12.4	16.5	13.6	3.2	− 9.9
	XGR	7.0	26.5	5.7	5.1	0.3	0.0	5.5	16.0	21.4	11.9	8.6	− 9.8
	CZR	7.0	26.9	6.5	6.3	0.5	0.0	6.7	19.2	25.9	6.0	4.3	− 9.8
	WGR	7.6	25.0	5.4	6.3	0.6	0.0	7.0	19.8	26.7	10.8	6.1	− 9.6
	LYR	7.9	26.9	5.5	3.7	0.2	0.0	3.8	15.6	19.4	6.0	2.1	0.0
	LHR	8.3	21.3	8.5	4.2	0.0	0.0	4.2	19.9	24.1	13.2	26.0	− 9.3
	NJLR	7.9	20.3	4.7	6.1	0.2	0.0	6.3	15.3	21.7	5.1	8.8	− 9.2
	TYR	6.9	25.1	8.0	3.4	0.1	0.0	3.5	5.6	9.1	22.1	− 9.3	− 10.2
DGR	1	6.6	20.4	9.7	2.1	0.3	0.0	2.5	9.4	11.9	9.7	3.5	−10.0
	2	7.0	22.1	5.5	3.6	0.0	0.0	3.6	15.1	18.8	9.8	1.9	−9.4
	3	7.6	23.2	4.3	4.0	0.1	0.0	4.1	12.4	16.5	6.7	− 4.8	−9.5
	4	7.0	19.8	6.9	4.0	0.1	0.0	4.1	18.2	22.3	11.5	0.7	−9.0
	5	7.6	26.3	5.3	4.2	0.1	0.0	4.2	8.7	13.0	21.6	8.4	−10.0
	6	7.2	24.0	4.3	3.7	0.1	0.0	3.8	12.3	16.1	8.4	6.8	−10.0
	7	7.4	26.1	9.7	5.0	0.1	0.0	5.1	16.2	21.3	11.9	13.6	−10.0
	8	7.0	25.1	5.8	3.2	0.0	0.0	3.3	7.9	11.2	6.6	15.6	−9.7
	9	8.0	26.1	4.7	3.9	0.3	0.0	4.2	10.6	14.9	11.4	0.6	−10.2
	10	8.2	25.5	8.2	4.4	0.1	0.1	4.6	13.3	17.9	15.4	9.7	−10.2
SGW	JWR watershed	5.3	16.3	1.6	10.6	0.1	0.0	10.7	0.2	10.9	8.2	5.2	− 10.0
	ZR watershed	5.2	15.1	2.4	27.3	0.7	0.0	27.9	0.7	28.6	10.0	4.7	− 10.0
	XGR watershed	6.3	14.3	2.3	121.4	0.6	0.0	122.0	0.5	122.5	7.9	0.7	− 10.0
	WGR watershed	6.6	14.1	0.3	77.2	0.1	0.0	77.2	3.0	80.2	3.0	3.4	− 9.0
	CZR watershed	4.3	16.5	4.1	91.2	0.2	0.1	91.5	0.1	91.6	5.0	1.1	− 10.1
	LYR watershed	4.3	13.2	2.5	51.9	1.1	0.0	53.0	3.5	56.5	3.9	− 1.9	− 11.2
	LHR watershed	7.4	16.2	5.2	97.7	1.7	0.0	99.3	2.6	101.9	4.3	11.9	− 8.7
	NJLR watershed	6.5	16.2	0.6	25.0	0.1	0.0	25.1	1.6	26.7	7.5	− 1.6	− 9.9
	TYR watershed	5.6	13.9	3.9	22.0	0.0	0.0	22.0	0.3	22.3	6.7	13.5	− 9.9

JWR Junwu River, *ZR* Zhu River, *CGR* Changguang River, *XGR* Xiaogu River, *WGR* Wugu River, *LYR* Luoyao River, *LHR* Liuhao River, *NJLR* Nanjiaolai River, *TYR* Taoyuan River, *CZR* Chengzi River, *SRs* sub-rivers, *SGW* groundwater in sub-watersheds

that of SRs (Table 2 and 3), which suggests that the degree of pollution is higher in groundwater than in surface water. This was not consistent with results reported by Zhang et al. (2014) in the North China Plain, with intensive maize and wheat farming, in which NO$_3^-$ concentrations of surface rivers were higher than that of groundwater.

The NO$_3^-$ concentrations of SGW in this coastal area were higher than those of other agricultural dominant regions in China, for example, 1.1 mg N L^{-1} in Loess Plateau (Xing and Liu 2016), ~35 mg N L^{-1} in Sichuang Province (Li et al. 2007), 0.1–19.4 mg N L^{-1} in the North China Plain (Zhang et al. 2014), and 0.3–17.6 mg N L^{-1} in the West lake watershed (Jin et al. 2015). Two primary reasons for the high NO$_3^-$ concentrations of SGW are application of fertilizer and agricultural managements. The amount of N fertilization used in the production of vegetables is ~200% higher than that

used for grain productions (Ju et al. 2009; Zhang et al. 2017; Kou et al. 2005; Shen et al. 2017). Overuse of fertilizers is common in agricultural productions in recent years (Zhang et al. 2015; Gong et al. 2011). The N use efficiency of vegetables is only ~14%, while the value of grains is as high as ~42% (Zhang et al. 2015). Therefore, the enhanced cultivation of vegetables in the study sub-watersheds possibly increased the N surplus in agricultural soils and increased the potential risk of N losses to surface water and groundwater. Primary agricultural management associated with NO$_3^-$ pollution of groundwater is irrigation. Flood groundwater irrigation is a general agricultural activity in the study area. The using volumes of water beyond the capacity of the crops and soil can lead to the leaching of excess irrigation water into groundwater under a flood irrigation pattern (Chen et al. 2017). The leaching process is a primary pathway for the transportation
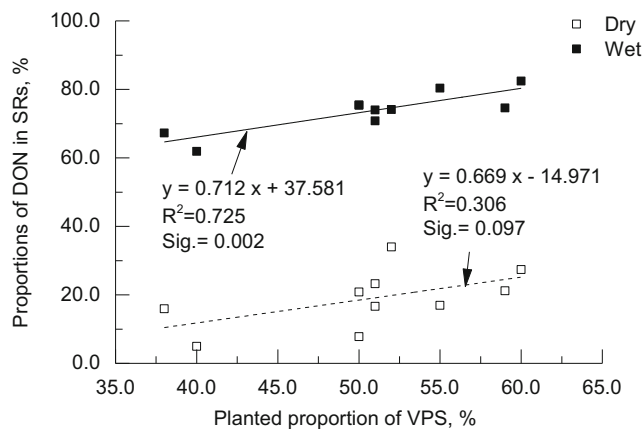
Fig. 5 Relationship between the proportions of DON in sub-rivers and proportions of MEC in sub-watersheds. Solid line denotes linear fit in the wet season, and dashed line denotes linear fit in the dry season. Abbreviations: MEC: modern economic crop rotation; SRs: sub-river in Dagu River

of dissolved N from surface soil to groundwater (Faccini et al. 2018; De Notaris et al. 2018). Wang and Zhu (2011) estimated that annual losses of NO_3^- through surface runoff and leaching were 0.9 and 33.5 kg N ha^{-1}, respectively. The same result was also found in the study of Salazar et al. (2019). Thus, increasing irrigation of agricultural productions possibly increases the possibility of dissolved N leaching into groundwater. Based on a household interview, the irrigation frequencies of VPS were obviously higher than those of GPS, except the natural rainfall. Thus, the enhanced cultivation of vegetables increases the dissolved N leaching into groundwater by increasing the N surplus in surface soil and irrigation frequencies.

Ammonium occupied a small percentage of DTN in SRs, DGR, and SGW (Fig. 4). In SRs, the NH_4^+ concentrations ranged from 0.1 to 2.7 mg N L^{-1} in the dry season and 0.0 to 1.4 mg N L^{-1} in the wet season. In DGR, the concentrations of NH_4^+ were 0.1–1.1 mg N L^{-1} in the dry season and 0.0–1.4 mg N L^{-1} in the wet season. Ammonium concentrations in SGW ranged from 0.0 to 0.3 mg N L^{-1} in the dry season and 0.1–0.8 mg N L^{-1} in the wet season (Table 2 and 3). According to the Environmental Quality Standards for Surface Water (GB3838-2002 China), water quality can be divided into five types based on the NH_4^+ concentration: I ≤ 0.15 mg N L^{-1}; II ≤ 0.5; III ≤ 1.0 mg N L^{-1}; IV ≤ 1.5 mg N L^{-1}; and V > 1.5 mg N L^{-1}. Most water aquatic systems in this study were type-II and type-III, indicating that NH_4^+ was not the dominant N species in the pollution of aquatic systems. MF application, which contains some ammonium, increases the NH_4^+ lost from agricultural land via surface runoff (Shan et al. 2015). However, NH_4^+ is easily adsorbed onto soil mineral and organic matter surfaces (Rosenfeld 1979); hence, it is usually not the dominant form of inorganic N in runoff.

The potential N losses to JZB via fluvial transport and submarine groundwater discharge

DGR is the largest channel for the transport of contaminants from watershed to seawater in the JZB area (Zhang 2007). Therefore, most N losses by surface runoff from agricultural lands in sub-watersheds would flow into DGR through the transport of SRs. The DTN concentrations of the DGR were 8.3–15.7 mg N L^{-1} and 11.2–22.3 mg N L^{-1} in the dry and wet seasons, respectively (Table 2 and 3). Like the changes in SRs, the dominant N species in DGR was NO_3^- in the dry and DON in the wet season (Fig. 4b). The NO_3^- concentration in DGR ranged from 7.8 to 13.8 mg N L^{-1} in the dry season, of which 60% of samples were over 10 mg N L^{-1}. The NO_3^- concentration decreased to 2.1–5.0 mg N L^{-1}, while the DON concentration increased to 7.9–18.2 mg N L^{-1} in the wet season (Table 2 and 3). DGR is a seasonal river, and primary flow fluxes happened in the wet season, whereas basic flows are only maintained in the dry season (Cui 2015). Therefore, DON is the dominant N forming losses from the DGR watershed to JZB, which is twice higher than the NO_3^- concentrations, via fluvial transport (Table 3 and Fig. 4b). Submarine groundwater discharge has been demonstrated as a significant channel for NO_3^- losses from watersheds to JZB (Qu et al. 2017). Even with certain seasonal changes, the high NO_3^- concentrations of groundwater in the dry season with 26.4–80.3 mg N L^{-1} and wet season with 10.6–121.4 mg N L^{-1} indicated that groundwater in the DGR watershed poses a huge potential NO_3^- source to JZB via submarine groundwater discharge, throughout the whole year.

Identification of potential NO_3^- sources and environmental behaviors

Identifying potential NO_3^- sources

As discussed above (Sect. 3.1.2), NO_3^- played a significant role in the pollution of surface water and groundwater in the study watershed and as a potential dominant N source entering JZB, via submarine groundwater discharge. The NO_3^- sources in the aquatic systems consisted of multiple sources, including CF, AD, manure and sewage (mostly MF), and SN. No simple mixing or only a single biological process is responsible for the shift in the N and O isotopic compositions of NO_3^- in aquatic systems (Xue et al. 2009). Based on the distinct $\delta^{15}N$ and $\delta^{18}O$ values of different NO_3^- sources (Table 4), we modified the classic dual biplot approach of Kendall et al. (2007) to identify potential NO_3^- sources in water aquatic systems in the watershed. In this study, the $\delta^{15}N$-NO_3^- values of the SRs, DGR, and SGW ranged from + 2.6 to +22.1, 0.3 to 21.6‰, and + 3.0 to + 15.7‰, respectively; the $\delta^{18}O$-NO_3^- values of SRs, DGR, and SGW are − 5.3 to +26.0‰, − 5.3 to +16.5‰, and − 5.3 to +13.5‰, respectively.

Table 4 The $\delta^{15}N$–NO_3^- and $\delta^{18}O$–NO_3^- of sources in the Dagu River watershed

Sources	Number	$\delta^{15}N$-NO_3^- (‰)		$\delta^{18}O$-NO_3^- (‰)		Shapiro–Wilk (sig.)	
		Ave ± SD	Reference range	Ave ± SD	Reference range	$\delta^{15}N$	$\delta^{18}O$
AD	6	+ 3.4 ± 2.4	− 13 to + 13[bc]	+ 21.3 ± 8.0	+ 8.6 to + 30.7	0.506	0.981
SN	6	+ 6.7 ± 1.3	0 to + 8[d]	+ 1.4 ± 0.3	− 10 to + 10[e]	0.987	0.429
CF	–	+ 0.2 ± 2.2[a]	− 6 to + 6[e]	+ 1.4 ± 0.3	− 10 to + 10[e]	–	0.429
MF	4	+ 12.5 ± 2.5	+ 4 to + 25[e]	+ 2.5 ± 2.2[a]	− 5 to + 10[e]	0.975	0.429

If sig. > 0.05, test distribution is normal

AD NO_3^- from atmosphere deposition, *SN* is NO_3^- derived from soil organic matter, *CF* NO_3^- derived from chemical fertilizer, *MF* NO_3^- derived from manure fertilizer, *Number* number of samples, *Ave* average value, *SD* standard deviation, – no measured value

[a] Li et al. 2013

[b] Heaton 1986

[c] Kendall 1998

[d] Xue et al. 2009

[e] Jr and Bonner 2010

All values of $\delta^{15}N$- and $\delta^{18}O$-NO_3^- in SRs, DGR, and SGW plot in the expected windows of AD, SN, CF, and MF (Fig. 6). This demonstrates that the NO_3^- concentrations in aquatic systems are mixtures of different sources. Most values fall into the windows of MF and SN, indicating that organic N might be the dominant NO_3^- source in aquatic systems. However, for some samples, the isotopic abundance plots lie in the overlap zone between the SN and MF source windows. Therefore, this result is inconclusive because the SGW has isotope signatures similar to those of MF and the isotopic composition of NO_3^- from CF could be modified by biological processes (such as nitrification and possibly denitrification) because

Fig. 6 Isotopic compositions of $\delta^{15}N$ and $\delta^{18}O$ in potential NO_3^- sources and samples in aquatic systems in the Dagu River watershed. Isotopic compositions of various sources in the diagram are modified after Kendall et al. (2007) and Xue et al. (2009). The limited lines of nitrification (+ 1.0‰ and + 12.1‰) are calculated by 1/3 of O-NO_3^- from atmosphere O_2 and 2/3 of O-NO_3^- from native H_2O ($\delta^{18}O$-NO_3^- = 1/3 $\delta^{18}O_2$ + 2/3 $\delta^{18}O$-H_2O), considering the 5–10‰ error (Aravena and Robertson 1998; Kendall 1998). Green solid line window presents manure fertilizer source, black and magenta dash line windows present chemical fertilizers, blue dash window presents soil organic nitrogen source, and red dash window presents atmosphere deposition. Abbreviations: DGR: Dagu River; SRs: sub-rivers of DGR; SGW: groundwater of sub-watersheds; AD: NO_3^- from atmosphere deposition; MF: NO_3^- from manure fertilizers; CF: NO_3^- from chemical fertilizer; SN: NO_3^- from soil organic matter
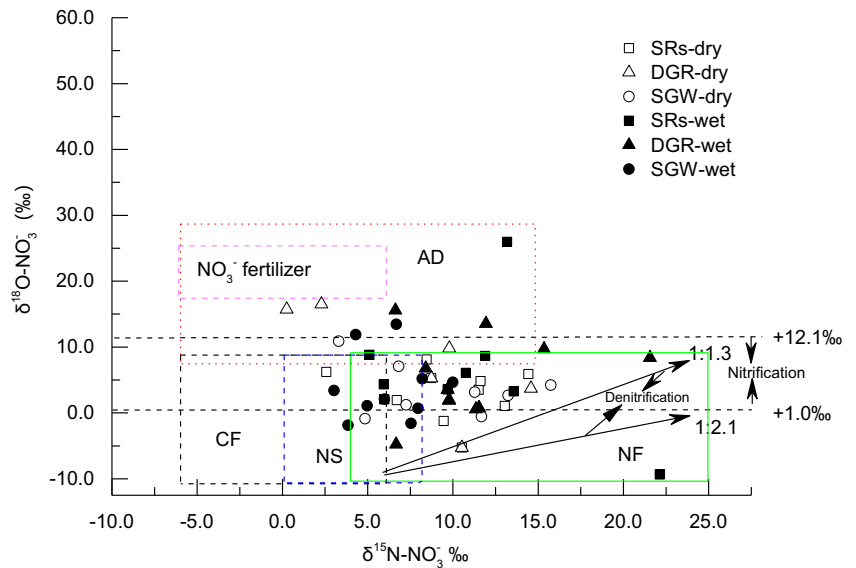
water from the soil and unsaturated zone flows into the rivers (Ding et al. 2015; Ji et al. 2017).

In SRs and DGR, the values of δ^{15}N-NO$_3^-$ were higher in the wet season (average + 11.2 ± 4.8‰, + 11.3 ± 4.2 ‰) than in the dry season (average + 9.7 ± 3.2‰, + 8.7 ± 4.0‰) (Table 2 and 3). This result can be attributed to the enhanced precipitation which carried more NO$_3^-$ from MF with higher high δ^{15}N values in the wet season. In comparison, the δ^{15}N-NO$_3^-$ of SGW decreased from the dry (+ 8.9 ± 4.0‰) to the wet season (+ 6.3 ± 2.2‰) (Table 2 and 3). This was caused by the application of CF, with lower δ^{15}N values, to agricultural lands in the wet season. The average δ^{18}O-NO$_3^-$ values were + 3.0 ± 3.8‰, + 5.4 ± 6.4‰, and + 3.3 ± 3.5‰ for SRs, the DGR, and SGW in the dry season, respectively, and + 5.7 ± 8.3‰, + 5.6 ± 6.0‰, and + 4.1 ± 5.2‰ in the wet season respectively (Table 2 and 3). The slight increasing values of δ^{18}O-NO$_3^-$ from the dry to wet seasons indicated the input of multiple NO$_3^-$ sources in combination with lower contributions from AD, which has high δ^{18}O values.

NO$_3^-$ environmental behaviors

Nitrification is an important process that transforms NH$_4^+$ into NO$_3^-$. Theoretically, 2/3 of the O atoms in NO$_3^-$ originate from the native ambient water and 1/3 are from atmospheric O$_2$ during microbial nitrification (Kendall 1998; Mayer et al. 2002; Xue et al. 2009). If no isotope fractionation occurs during O incorporation, the δ^{18}O-NO$_3^-$ value of the newly produced NO$_3^-$ can be calculated from the known δ^{18}O values of atmospheric O$_2$ and ambient water. In this study, the δ^{18}O-H$_2$O values of SRs, DGR, and SGW range from − 10.26 to − 8.63‰, − 10.37 to − 9.00‰, and − 11.23 to −8.89‰, respectively, with slight differences among the aquatic systems (Table 2 and 3). Therefore, we used values between − 11.2 and − 8.7‰ as the native δ^{18}O-H$_2$O and used the default value of + 23.5‰ in the atmosphere as δ^{18}O-O$_2$ (Kroopnick and Craig 1972; Hollocher 1984) to calculate the range of δ^{18}O-NO$_3^-$ from nitrification in the DGR watershed. If the O-NO$_3^-$ from these two sources is incorporated without isotope fractionation, the range of the δ^{18}O-NO$_3^-$ from nitrification is + 1.0 to + 2.1‰. Because of complex factors affecting nitrification, for instance, (1) the δ^{18}O value of the soil O$_2$ is higher than that of atmospheric O$_2$ due to O isotope fractionation during respiration, (2) significant isotope fractionation occurs during the incorporation of oxygen from H$_2$O and O$_2$ in newly formed NO$_3^-$, and (3) the ratio of oxygen incorporation from H$_2$O and O$_2$ is not 2:1; the δ^{18}O value of microbially produced NO$_3^-$ is up to 5–10‰ higher than the calculated theoretical maximum (Aravena and Robertson 1998; Kendall 1998). In addition, evaporation can also elevate the δ^{18}O-H$_2$O and thus the δ^{18}O-NO$_3^-$ value produced by nitrification. However, no notable δ^{18}O-H$_2$O enhancement was observed in different aquatic systems and in different seasons in this study

(Table 2). This indicates that evaporation insignificantly influences the δ^{18}O value of NO$_3^-$ from nitrification production in the DGR watershed. Therefore, we introduce the minimum of 1.0‰ and maximum of 12.1‰ as the theoretical range of δ^{18}O-NO$_3^-$ produced by nitrification (Fig. 6). In this study, the NO$_3^-$ in 100% of the SRW samples obtained during the dry season and in 80% of the samples obtained during the wet season is intermediate between the ranges of the nitrification-associated NO$_3^-$; the value of SGW is 80% and 70% in the dry and wet seasons, respectively. This indicated that most of NO$_3^-$ derived from MF and SN via microbial activities with nitrification rather than from CF and AD, directly.

Denitrification is an important mechanism for the reduction of the NO$_3^-$ concentrations in aquatic environments via the transformation of dissolved NO$_3^-$ to N$_2$ or N$_2$O (Well and Flessa 2009; Yin et al. 2017). By preferentially reducing light isotopes, denitrification usually causes isotopic enrichment of δ^{15}N and δ^{18}O in the residual NO$_3^-$ (Böttcher et al. 1990; Aravena and Robertson 1998). A linear relationship indicates the enrichment of δ^{15}N-NO$_3^-$ relative to δ^{18}O-NO$_3^-$ by a factor ranging from 1.3 to 2.1:1, providing evidence for denitrification (Aravena and Robertson 1998; Xue et al. 2009). In this study, the enrichments were not observed between δ^{15}N-NO$_3^-$ and δ^{18}O-NO$_3^-$ of SR, DGR, and SGW in both the dry and wet seasons (Fig. 6). Thus, the residual NO$_3^-$ during denitrification could be minor in the DGR watershed. There was no simple linear correlation between the δ^{15}N and δ^{18}O-NO$_3^-$ values in ten sampling sites of SRs, ten sampling sites of DGR, and nine sampling sites of SGW, respectively (Fig. 6). Previous studies demonstrated that the residual logarithm of NO$_3^-$ concentrations has a negative relationship with the values of δ^{15}N or δ^{18}O in the residual NO$_3^-$ if denitrification occurs in agricultural dominated watersheds (Wei et al. 2015; Xu et al. 2016). In this study, this relationship was not obvious between the isotopes of NO$_3^-$ and ln[NO$_3^-$] among SRs, DGR, and SGW in both wet and dry seasons (Fig. 7). All these results indicated that denitrification is insignificant for the deletion NO$_3^-$ of water and disturbance isotopic compositions of NO$_3^-$ in the study area. SRs and DGR are totally open oxygen systems, and the DO concentrations range from 3.0 to 9.7 mg L^{-1} (Table 2 and 3), which is too high for denitrification (Yin et al. 2017). The SGW may satisfy the requirements for DO concentrations for denitrification. However, the DOC concentration of SGW in the watershed is only 0.01–0.05 mg L^{-1}. The experimental reduction of nitrate in SGW samples leads to no notable denitrification under anaerobic conditions. Possibly, this is attributed to the lack of electron donors for denitrification at a low DOC concentration (Well and Flessa 2009; Vidal-Gavilan et al. 2013). Therefore, denitrification is insignificant for isotopic fractionation of NO$_3^-$ both in surface water and groundwater and multiple sources might be the main reason for the δ^{15}N and δ^{18}O-NO$_3^-$ compositions. In addition, the weak denitrification indicates that

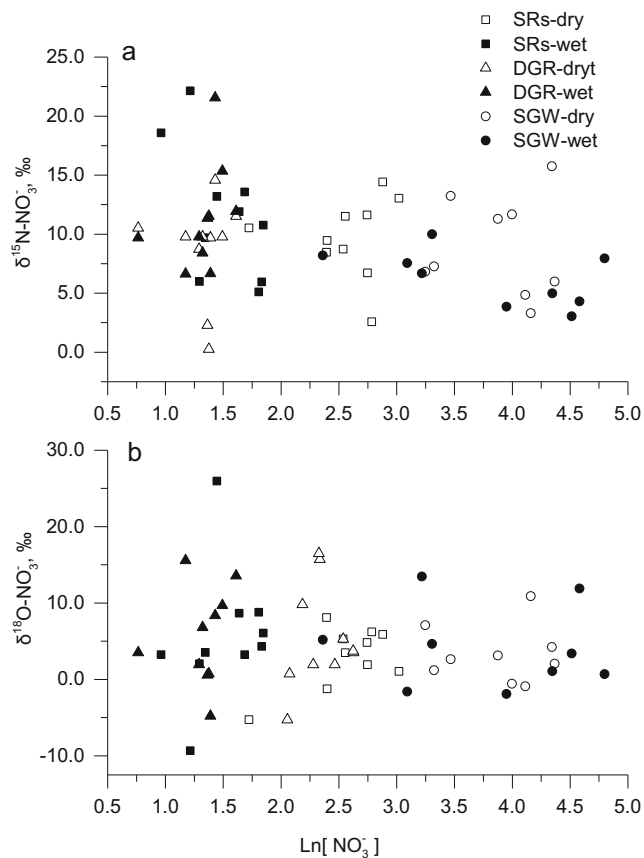**Fig. 7** The relationship between ln[NO_3^-] and **a** δ^{15}N-NO_3^- and **b** δ^{18}O-NO_3^- in aquatic systems. Abbreviations: DGR: Dagu River; SRs: sub-river of Dagu River; SGW: groundwater in sub-watersheds

the aquatic systems possibly lack a self-cleaning capacity based on biological activities. Thus, external anthropic favors should be provided to govern and protect the quality of aquatic systems in the watershed.

Quantitative analysis of potential NO_3^- sources from the watershed to JZB

Based on the dual-plot approach, potential NO_3^- sources include AD, CF, SN, and MF in the DGR watershed (Fig. 6). We introduced a SIAR mixing model to estimate the contribution of each potential source to the NO_3^- concentrations in the three aquatic systems. In this study, the δ^{15}N and δ^{18}O values of different sources were used as site-specific isotope values. Table 4 shows the ranges of the δ^{15}N and δ^{18}O values of the four potential NO_3^- sources in the DGR watershed. The δ^{15}N and δ^{18}O-NO_3^- values of the AD, CF, NS, and MF are within the typical δ^{15}N and δ^{18}O ranges of various natural and anthropogenic NO_3^- sources. The results of the Shapiro–Wilk test for normality show that the δ^{15}N and δ^{18}O values of the potential sources are normally distributed. The δ^{18}O values of the SN and CF sources were not directly measured; we used the value of +

1.4‰ ± 0.3‰ from microbial nitrification. As δ^{15}N values from CF, we used the results of + 0.2‰ ± 2.2‰ for Weifang city (Li et al. 2013), which is close to the study area and is based on a similar fertilizer application. The δ^{15}N-NO_3^- and δ^{18}O-NO_3^- values of SRs, DGR, and SGW were determined in both dry and wet seasons. In addition, we assumed a fractionation factor $c_{jk} = 0$ because of the weak denitrification in the aquatic systems (as discussed in Sect. 3.2.2).

Different sources have various contributions to NO_3^- in the aquatic systems (Table 5). The results show that MF contributed over 20% of NO_3^- in aquatic systems. In the DGR, MF contributed 52.6% and 69.0% to the NO_3^- concentrations in the DGR in the dry and wet seasons, respectively. In SRs, the contribution of MF ranged from 21.5 to 54.1%, while the values ranged from 20.6 to 54.6% in SGW. SN is another primary source of NO_3^- in aquatic systems in the watershed. In DGR, SN contributed 34.1% and 20.6% of NO_3^- in the dry and wet seasons, respectively. In SGW, 27.6–53.0% and 28.9–48.5% of NO_3^- were attributable to SN in the dry and wet seasons, respectively. In SRs, 27.0–53.8% and 19.5–53.2% of NO_3^- were attributable to SN in the dry and wet seasons, respectively. These findings indicate that reduced nitrification in the soil zones (including SN and MF) of the heavily fertilized field was the main NO_3^- source in aquatic systems throughout the year. The result was consistent with the enhanced cultivation of vegetables, which increased MF application to agricultural soil.

In this study, the contributions of CF to NO_3^- in SGW (6.7–34.3%) were higher than that to NO_3^- in SRs (5.5–23.9%). For instance, the CF contributed 34.3% of NO_3^- in the SGW in the LHR sub-watershed during the dry season and only 23.9% in the wet season. CF often directly contributed NO_3^- with a high freedom of transport in water aquatic systems (Meybeck 1982). In agricultural lands, the NO_3^- losses via leaching into groundwater were obviously higher than NO_3^- losses via surface runoff to surface water (Wang and Zhu 2011; and Salazar et al. 2019). This process would be continuing deterioration due to the enhanced cultivation of vegetables as discussed in Sect. 3.1.2. AD contributed least to NO_3^- in the three aquatic systems. The contributions of AD were 2.8–8.5% of NO_3^- in SRs and 1.6–8.7% of NO_3^- in SGW during the dry season, and the values change to 3.1–18.8% in SRs and 3.9–18.2% in SGW during the wet season. The increasing contributions of AD are likely to be attributed to because of the increased precipitation during the wet season, which carries the NO_3^- of atmosphere into surface water and groundwater. However, the contribution of AD to NO_3^- in DGR is ~ 4% without distinctive differences between the wet and dry seasons. Possibly, this attributed to the NO_3^- concentrations of DGR which are a mixture of NO_3^- and SRs, which diluted the contributions of AD.

Based on the SIAR, the contribution of each NO_3^- source in the aquatic systems is quantified, which is in

Table 5 The concentrations of potential NO$_3^-$ sources of aquatic systems in the DGR watershed

Samples		Dry								Wet							
		AD		SN		CF		MF		AD		SN		CF		MF	
		Average %	95%	Average	95%	Average	95%	Average	95%	Average %	95%	Average	95%	Average	95%	Average	95%
SRs	JWR	2.8	0–10.8	46.2	12.5–78.5	5.5	0–18.7	45.5	17.7–74.9	7.9	0–28.0	32.2	1.0–58.9	11.4	0–33.5	48.5	15.8–82.1
	CGR	2.7	0–8.7	43.9	1.9–85.7	6.2	0–18.3	47.2	6.4–87.7	10.4	0–33.8	29.4	0–58.8	15.2	0–39.7	45	5.5–87.2
	ZR	4.1	0–9.0	41.4	13.8–69.5	11.6	0–23.2	42.9	16.8–70.4	10	0–32.8	30	0–59.8	15.1	0–40.3	44.9	6.8–86.7
	XGR	8.2	0–29.2	29	0–56.4	12.1	0–36.0	50.7	13.5–88.8	4.4	0–9.9	35.8	2.1–68.8	13.2	0–25.7	46.6	11.0–81.2
	CZR	4.4	0–18.8	34	0.4–63.9	7.5	0–28.1	54.1	18.3–90.4	11.3	0–34.8	41.4	4.6–80.7	16.7	0–37.6	30.6	5.1–54.3
	WGR	3.1	0–36.3	28.2	0–55.4	17.1	0–41.0	51.6	4.1–82.1	3.1	0–7.3	40.1	1.7–77.0	5.9	0–15.4	50.9	14.2–87.7
	LYR	3.6	0–36.2	34.7	1.8–65.2	17.7	0–37.7	44	11.1–57.2	14.9	0–26.5	34.9	1.7–67.3	20	0–39.9	30.2	7.6–51.9
	LHR	8.5	0–35.2	53.8	12.7–95.8	16.2	0–48.6	21.5	0–49.2	12.9	0.7–22.7	19.5	0–40.7	23.9	0–47.7	43.7	20.3–66.4
	NJLR	5.5	0–25.0	29.5	0.4–54.8	14.9	0–37.7	50.1	11.5–73.7	3.9	0–10.4	53.2	25.0–81.0	18.4	1.0–31.4	24.5	1.3–46.7
	TYR	1.5	0–18.3	27	0–52.2	16.8	0–40.1	54.7	5.6–74.8	18.8	0–41.9	28	0–53.8	22.3	0–45.7	30.9	0–59.5
DGR		4.1	0–10.8	34.1	2.2–62.1	9.2	0–24.0	52.6	24.6–82.5	3.7	0–9.7	20.6	0–49.9	6.7	0–18.3	69	37.5–94.7
SGW	JWR watershed	1.6	0–15.6	33.1	1.4–61.7	16.5	0–36.7	48.8	33.0–60.4	3.9	0–17.0	48.5	11.7–85.3	6.7	0–24.9	40.9	10.7–68.9
	ZR watershed	1.8	0–13.8	29	0–57.5	15.8	0–39.7	53.4	16.0–86.1	4.2	0–17.5	35.9	2.3–65.2	7.1	0–24.4	52.8	22.2–87.1
	XGR watershed	8.7	0–21.1	28.8	0–57.0	12.5	0–35.8	50	12.3–87.6	12.7	0–34.9	32.8	1.6–60.0	15.5	0–36.4	39	14.0–63.9
	WGR watershed	1.3	0–15.8	27.6	0–53.7	16.5	0–40.0	54.6	6.1–80.6	7.5	0–21.8	33.8	1.0–64.2	31.2	1.9–54.5	27.5	10.6–40.4
	CZR watershed	1.3	0–7.8	34.5	1.4–67.2	20.1	1.6–40.0	44.1	37.5–51.7	18.2	0–40.4	33.3	1.1–63.9	23.9	0.4–44.0	24.6	2.5–45.1
	LYR watershed	1.5	0–11.0	32.5	1.2–62.2	22.1	1.0–45.0	43.9	25.4–43.8	16.8	0–33.5	31.8	1.2–60.3	28.8	2.6–50.3	22.6	6.9–38.0
	LHR watershed	3.5	0–9.6	37.5	10.4–71.2	31.5	13.8–43.8	27.5	9.8–40.2	4.7	0–12.4	40.4	14.8–64.0	34.3	15.7–48.9	20.6	0.9–40.0
	TYR watershed	8.2	0–30.8	32.2	0–62.9	13.3	0–38.1	46.3	9.1–90.9	10.4	0–21.2	28.9	1.8–51.6	27.9	2.1–51.5	32.8	11.8–54.1
	NJLR watershed	3.5	0–10.1	53	36.0–65.0	9.3	0–38.4	34.2	6.3–87.8	14.6	0–36.5	31.6	1.2–57.9	16.9	0–38.3	36.9	11.6–60.4

95% is the confidence interval calculated by SIAR

AD NO$_3^-$ from atmosphere deposition, *MF* NO$_3^-$ from manure and sewage, *CF* NO$_3^-$ from chemical fertilizer, *SN* NO$_3^-$ from soil organic matter, *JWR* Junwu River, *ZR* Zhu River, *CGR* Changguang River, *XGR* Xiaogu River, *WGR* Wugu River, *LYR* Luoyao River, *LHR* Liuhao River, *NJLR* Nanjiaolai River, *TYR* Taoyuan River, *CZR* Chengzi River, *SRs* sub-rivers, *SGW* groundwater in sub-watersheds

accordance with the results obtained using the dual-plot approach. However, the SIAR model provides a more accurate quantification of each potential NO_3^- source than the dual-plot approach. The results suggest that the MF is the dominant nitrate source, followed by SN, CF, and AD, in the aquatic systems of the watershed. However, certain factors could introduce uncertainty into the SIAR model. A wide range of individual source contributions is observed in the SIAR results. Therefore, more samples need to be collected to obtain a more accurate contribution estimate using the SIAR mixing model. Furthermore, small variations in the isotope values of the samples might result in significant changes in the source apportionment, as estimated using SIAR. Thus, additional water samples and native source samples might be required to reduce the uncertainty.

Conclusion

Agricultural land is the primary origin of the N loads entering both surface water and groundwater in the JZB area. The production of vegetables is likely to be responsible for the increased loss of DON from the watershed to JZB via the DGR, transport, and accelerated risk of NO_3^- discharge with the seawater of JZB, due to the enhanced production of vegetables in the watershed scale. The isotopic compositions of NO_3^- indicated that most NO_3^- derived from fertilizer application, rather than directly from AD. This suggests that the production of vegetables possibly increased excess NO_3^- in surface soil which contributes to the deterioration of groundwater quality in the JZB area. The high concentration of NO_3^- in surface rivers in the dry season was mainly derived from the high DON during the wet season. This study confirmed that the management of crop productions and reasonable MF application should be implemented to protect the quality of aquatic systems in the JZB area. This study also improves our understanding of N loads and NO_3^- pollution of the aquatic system in agricultural watersheds and provides a fundamental basis for planning sustainable agricultural production without adverse impacts on the environment in the future.

Compliance with ethical standards

Conflict of interest The authors declare no conflict of interest.

References

Amberger A, Schmidt HL (1987) Natürliche Isotopengehalte von Nitrat als Indikatoren für dessen Herkunft. Geochim Cosmochim Acta 51: 2699–2705. https://doi.org/10.1016/0016-7037(87)90150-5

Aravena R, Robertson WD (1998) Use of multiple isotope tracers to evaluate denitrification in ground water: study of nitrate from a large-flux septic system plume. Groundwater 36:975–982. https://doi.org/10.1111/j.1745-6584.1998.tb02104.x

Babiker IS, Mohamed MA, Terao H, Kato K, Ohta K (2004) Assessment of groundwater contamination by nitrate leaching from intensive vegetable cultivation using geographical information system. Environ Int 29:1009–1017. https://doi.org/10.1016/S0160-4120(03)00095-3

Böttcher J, Strebel O, Voerkelius S, Schmidt H-L (1990) Using isotope fractionation of nitrate-nitrogen and nitrate-oxygen for evaluation of microbial denitrification in a sandy aquifer. J Hydrol 114:413–424. https://doi.org/10.1016/0022-1694(90)90068-9.

Chen S, Sun C, Wu W, Sun C (2017) Water leakage and nitrate leaching characteristics in the winter wheat–summer maize rotation system in the North China Plain under different irrigation and fertilization management practices. Water 9:141. https://doi.org/10.3390/w9020141

Choi W-J, Kwak J-H, Lim S-S, Park H-J, Chang SX, Lee S-M, Arshad MA, Yun S-I, Kim H-Y (2017) Synthetic fertilizer and livestock manure differently affect $\delta^{15}N$ in the agricultural landscape: a review. Agric Ecosyst Environ 237:1–15. https://doi.org/10.1016/j.agee.2016.12.020

Crawford J, Hollins SE, Meredith KT, Hughes CE (2017) Precipitation stable isotope variability and subcloud evaporation processes in a semi-arid region. Hydrol Process 31:20–34. https://doi.org/10.1002/hyp.10885

Cui SF, (2015) Combined simulation and prediction of surface water and groundwater in dagu river basin under changing environment [D]. Shandong Normal University

De Notaris C, Rasmussen J, Sørensen P, Olesen JE (2018) Nitrogen leaching: a crop rotation perspective on the effect of N surplus, field management and use of catch crops. Agric Ecosyst Environ 255:1–11. https://doi.org/10.1016/j.agee.2017.12.009

D'Elia CF, Steudler PA (1977) Determination of total nitrogen in aqueous samples using persulfate digestion 1. Limnol Oceanogr 22:760–764. https://doi.org/10.4319/lo.1977.22.4.0760.

Ding J, Xi B, Xu Q, Su J, Huo S, Liu H, Yu Y, Zhang Y (2015) Assessment of the sources and transformations of nitrogen in a plain river network region using a stable isotope approach. J Environ Sci 30:198–206. https://doi.org/10.1016/j.jes.2014.05.053

Faccini B, Di Giuseppe D, Ferretti G, Coltorti M, Colombani N, Mastrocicco M (2018) Natural and NH4+-enriched zeolitite amendment effects on nitrate leaching from a reclaimed agricultural soil (Ferrara Province, Italy). Nutr Cycl Agroecosyst 110:327–341. https://doi.org/10.1007/s10705-017-9904-4

Filoso S, Martinelli LA, Williams MR, Lara LB, Krusche A, Ballester MV, Victoria R, Camargo PBD (2003) Land use and nitrogen export in the Piracicaba River basin, Southeast Brazil. Biogeochemistry 65: 275–294. https://doi.org/10.1023/A:1026259929269

García-Díaz A, Bienes R, Sastre B, Novara A, Gristina L, Cerdà A (2017) Nitrogen losses in vineyards under different types of soil groundcover. A field runoff simulator approach in central Spain. Agric Ecosyst Environ 236:256–267. https://doi.org/10.1016/j.agee.2016.12.013

Goldman E, Jacobs R (1961) Determination of nitrates by ultraviolet absorption. Journal 53:187–191. https://doi.org/10.1002/j.1551-8833.1961.tb00651.x

Gong P, Liang L, Zhang Q (2011) China must reduce fertilizer use too. Nature 473:284–285

Han Y, Fan Y, Yang P, Wang X, Wang Y, Tian J, Xu L, Wang C (2014) Net anthropogenic nitrogen inputs (NANI) index application in Mainland China. Geoderma 213:87–94. https://doi.org/10.1016/j.geoderma.2013.07.019

Heaton THE (1986) Isotopic studies of nitrogen pollution in the hydrosphere and atmosphere: a review. Chem Geol Isot Geosci 59:87–102. https://doi.org/10.1016/0168-9622(86)90059-X

Hollocher TC (1984) Source of the oxygen atoms of nitrate in the oxidation of nitrite by nitrobacter agilis and evidence against a P-O-N anhydride mechanism in oxidative phosphorylation. Arch Biochem Biophys 233:721–727. https://doi.org/10.1016/0003-9861(84)90499-5

Howarth RW (2008) Coastal nitrogen pollution: a review of sources and trends globally and regionally. Harmful Algae 8:14–20. https://doi.org/10.1016/j.hal.2008.08.015

Ji X, Xie R, Hao Y, Lu J (2017) Quantitative identification of nitrate pollution sources and uncertainty analysis based on dual isotope approach in an agricultural watershed. Environ Pollut 229:586–594. https://doi.org/10.1016/j.envpol.2017.06.100

Jin J, Liu SM, Ren JL, Liu CG, Zhang J, Zhang GL, Huang DJ (2013) Nutrient dynamics and coupling with phytoplankton species composition during the spring blooms in the Yellow Sea. Deep-Sea Res Part II:Topical Stud Oceanogr 97:16–32. https://doi.org/10.1016/j.hal.2008.08.015

Jr WJF, Bonner FT (2010) Nitrogen-isotope ratios of nitrate in ground water under fertilized fields, Long Island, New York. Groundwater 23:59–67. https://doi.org/10.1111/j.1745-6584.1985.tb02780.x

Ju XT, Xing GX, Chen XP, Zhang SL, Zhang LJ, Liu XJ, Cui ZL, Yin B, Christie P, Zhu ZL (2009) Reducing environmental risk by improving N management in intensive Chinese agricultural systems. Proc Natl Acad Sci U S A 106:3041–3046. https://doi.org/10.1073/pnas.0902655106

Kang X, Song J, Yuan H, Li X, Li N, Duan L (2017) The sources and composition of organic matter in sediments of the Jiaozhou Bay: implications for environmental changes on a centennial time scale. Acta Oceanol Sin 36:68–78. https://doi.org/10.1007/s13131-017-1076-1

Kendall C (1998) Isotope tracers in catchment hydrology 1st Edition. Environ Earth Sci.

Kendall C, Elliott EM, and Wankel SD, (2007) Tracing anthropogenic inputs of nitrogen to ecosystems, chapter 12, In: Michener RH and Lajtha K (Eds.), Stable isotopes in ecology and environmental science, 2nd edition, Blackwell Publishing, p. 375–449

Korth F, Deutsch B, Frey C, Moros C, Voss M (2014) Nitrate source identification in the Baltic Sea using its isotopic ratios in combination with a Bayesian isotope mixing model. Biogeosciences 11:4913–4924

Kou C, Ju X, Zhang F (2005) Nitrogen balance and its effects on nitrate-N concentration of groundwater in three intensive cropping systems of North China. Chin J Appl Ecol 16:660–667. https://doi.org/10.13287/j.10019932.2005.0015

Kroopnick P, Craig H (1972) Atmospheric oxygen: isotopic composition and solubility fractionation. Science 175:54–55. https://doi.org/10.1126/science.175.4017.54

Li Y Z (2014) The evolution of spatial layout of China's crop farming (1978–2009) [D], China Agricultural University

Li X, Masuda H, Koba K, Zeng H (2007) Nitrogen isotope study on nitrate-contaminated groundwater in the Sichuan Basin, China. Water Air Soil Pollut 178:145–156. https://doi.org/10.1007/s11270-006-9186-y

Li YZ, Jia XF, Xu CY, Wang QS, Li QZ (2013) Study on the nitrate sources in groundwater in Shandong province. Ecol Environ Sci 22(8):1401–1407. https://doi.org/10.16258/j.cnki.1674-5906.2013.08.026

Liu SM, Li LW, Zhang GL, Liu Z, Yu Z, Ren JL (2012) Impacts of human activities on nutrient transports in the Huanghe (Yellow River) estuary. J Hydrol 430-431:103–110. https://doi.org/10.1016/j.jhydrol.2012.02.005

Lv C (2011) The study on the formation of the main vegetable production areas and the economic effect in China. [D], Nanjing Agricultural University.

Manninen N, Soinne H, Lemola R, Hoikkala L, Turtola E (2018) Effects of agricultural land use on dissolved organic carbon and nitrogen in surface runoff and subsurface drainage. Sci Total Environ 618:1519–1528. https://doi.org/10.1016/j.scitotenv.2017.09.319

Mayer B, Boyer EW, Goodale C, Jaworski NA, Nvan B, Howarth RW, Seitzinger S, Billen G, Lajtha K, Nadelhoffer K (2002) Sources of nitrate in rivers draining sixteen watersheds in the northeastern U.S.: isotopic constraints. Biogeochemistry 57(58):171–197. https://doi.org/10.1023/A:1015744002496

Mckenzie VJ, Townsend AR (2007) Parasitic and infectious disease responses to changing global nutrient cycles. Ecohealth 4:384–396. https://doi.org/10.1007/s10393-007-0131-3

Meybeck M (1982) Carbon, nitrogen, and phosphorous transport by world rivers. Am.J.Sci 282:401–450. https://doi.org/10.2475/ajs.282.4.401

National Earth System Science Data Sharing Infrastructure http://www.geodata.cn/Accessed 2015

GB 7479-87, (1987) Water quality - Determination of ammonium-Nessler's reagent colorimetric method (National standard method, China). National Environmental Protection Agency

Oelmann Y, Kreutziger Y, Bol R, Wilcke W (2007) Nitrate leaching in soil: tracing the NO3− sources with the help of stable N and O isotopes. Soil Biol Biochem 39:3024–3033. https://doi.org/10.1016/j.soilbio.2007.05.036

Parnell AL, Jackson A, 2008. SIAR: stable isotope analysis in R Available from: http://cran.r-project.org/web/packages/siar/index.htmlAccesses 2016

Parnell A, Phillips DL, Bearhop S, Semmens B, Ward EJ, MooreW, Jackson AJ, Grey J, Kelly D, Inger R (2013) Bayesian Stable Isotope Mixing Models.

Qu W, Li H, Huang H, Zheng C, Wang C, Wang X, Zhang Y (2017) Seawater-groundwater exchange and nutrients carried by submarine groundwater discharge in different types of wetlands at Jiaozhou Bay, China. J Hydrol 555:185–197. https://doi.org/10.1016/j.jhydrol.2017.10.014

Rosenfeld JK (1979) Ammonium adsorption in nearshore anoxic sediments. Limnol Oceanogr 24:356–364. https://doi.org/10.4319/lo.1979.24.2.0356

Russo TA, Tully K, Palm C, Neill C (2017) Leaching losses from Kenyan maize cropland receiving different rates of nitrogen fertilizer. Nutr Cycl Agroecosyst 108:195–209. https://doi.org/10.1007/s10705-017-9852-z

Salazar O, Balboa L, Peralta K, Rossi M, Casanova M, Tapia Y, Singh R, Quemada M (2019) Effect of cover crops on leaching of dissolved organic nitrogen and carbon in a maize-cover crop rotation in Mediterranean Central Chile. Agric Water Manag 212:399–406. https://doi.org/10.1016/j.agwat.2018.07.031

Shan L, He Y, Chen J, Huang Q, Lian X, Wang H, Liu Y (2015) Nitrogen surface runoff losses from a Chinese cabbage field under different nitrogen treatments in the Taihu Lake Basin, China. Agric Water Manag 159:255–263. https://doi.org/10.1016/j.agwat.2015.06.008

Shen LD, Wu HS, Liu X, Li J (2017) Vertical distribution and activity of anaerobic ammonium-oxidising bacteria in a vegetable field. Geoderma 288:56–63. https://doi.org/10.1016/j.geoderma.2016.11.007

Sigman DM, Casciotti KL, Andreani M, Barford C, Galanter M, Böhlke JK (2001) A bacterial method for the nitrogen isotopic analysis of nitrate in seawater and freshwater. Anal Chem 73:4145–4153. https://doi.org/10.1021/ac010088e

Trivelin PCO, Oliveira MWD, Vitti AC, Gava GJDC, Bendassolli JA (2002) Nitrogen losses of applied urea in the soil-plant system

during two sugar cane cycles. Pesq Agrop Brasileira 37:193–201. https://doi.org/10.1590/S0100-204X2002000200011

Vidal-Gavilan G, Folch A, Otero N, Solanas AM, Soler A (2013) Isotope characterization of an in situ biodenitrification pilot-test in a fractured aquifer. Appl Geochem 32:153–163. https://doi.org/10.1016/j.apgeochem.2012.10.033

Wang T, Zhu B (2011) Nitrate loss via overland flow and interflow from a sloped farmland in the hilly area of purple soil, China. Nutr Cycl Agroecosyst 90:309–319. https://doi.org/10.1007/s10705-011-9431-7

Wang J, Yan W, Chen N, Li X, Liu L (2015) Modeled long-term changes of DIN:DIP ratio in the Changjiang River in relation to Chl-α and DO concentrations in adjacent estuary. Estuar Coast Shelf Sci 166:153–160. https://doi.org/10.1016/j.ecss.2014.11.028

Wang W, Wu X, Yin C, Xie X (2019) Nutrition loss through surface runoff from slope lands and its implications for agricultural management. Agric Water Manag 212:226–231. https://doi.org/10.1016/j.agwat.2018.09.007

Wei WW, Grace MR, Cartwright I, Cook PLM (2015) Unravelling the origin and fate of nitrate in an agricultural–urban coastal aquifer. Biogeochemistry 122:343–360. https://doi.org/10.1007/s10533-014-0045-4

Well R, Flessa H (2009) Isotopologue signatures of N₂O produced by denitrification in soils. J Geophys Res: Biogeosciences 114. doi: https://doi.org/10.1029/2008jg000804

Winings JH, Yin X, Agyin-Birikorang S, Singh U, Sanabria J, Savoy HJ, Allen FL, Saxton AM (2017) Agronomic effectiveness of an organically enhanced nitrogen fertilizer. Nutr Cycl Agroecosyst 108:149–161. https://doi.org/10.1007/s10705-017-9846-x

Wolters J-W, Gillis LG, Bouma TJ, van Katwijk MM, Ziegler AD (2016) Land use effects on mangrove nutrient status in Phang Nga Bay, Thailand. Land Degrad Dev 27:68–76. https://doi.org/10.1002/ldr.2430

Xing M, Liu W (2016) Using dual isotopes to identify sources and transformations of nitrogen in water catchments with different land uses, Loess Plateau of China. Environ Sci Pollut Res 23:388–401. https://doi.org/10.1007/s11356-015-5268-y

Xu S, Kang P, Sun Y (2016) A stable isotope approach and its application for identifying nitrate source and transformation process in water. Environ Sci Pollut Res Int 23:1133–1148. https://doi.org/10.1007/s11356-015-5309-6

Xue D, Botte J, De BB, Accoe F, Nestler A, Taylor P, Van CO, Berglund M, Boeckx P (2009) Present limitations and future prospects of stable isotope methods for nitrate source identification in surface and groundwater. Water Res 43:1159–1170. https://doi.org/10.1016/j.watres.2008.12.048

Yan W, Mayorga E, Li X, Seitzinger SP, Bouwman AF (2010) Increasing anthropogenic nitrogen inputs and riverine DIN exports from the Changjiang River basin under changing human pressures. Glob Biogeochem Cycles 24. doi: https://doi.org/10.1029/2009GB003575

Yaşar Korkanç S, Dorum G (2019) The nutrient and carbon losses of soils from different land cover systems under simulated rainfall conditions. CATENA 172:203–211. https://doi.org/10.1016/j.catena.2018.08.033

Yi B, Zhang Q, Gu C, Li J, Abbas T, Di H (2018) Effects of different fertilization regimes on nitrogen and phosphorus losses by surface runoff and bacterial community in a vegetable soil. J Soils Sediments 18:3186–3196. https://doi.org/10.1007/s11368-018-1991-6

Yin G, Hou L, Liu M, Zheng Y, Li X, Lin X, Gao J, Jiang X, Wang R, Yu C (2017) Effects of multiple antibiotics exposure on denitrification process in the Yangtze Estuary sediments. Chemosphere 171:118–125. https://doi.org/10.1016/j.chemosphere.2016.12.068

Yu D, Yan W, Chen N, Peng B, Hong H, Zhuo G (2015) Modeling increased riverine nitrogen export: source tracking and integrated watershed-coast management. Mar Pollut Bull 101:642–652. https://doi.org/10.1016/j.marpolbul.2015.10.035

Yuan Y, Song D, Wu W, Liang S, Wang Y, Ren Z (2016) The impact of anthropogenic activities on marine environment in Jiaozhou Bay, Qingdao, China: a review and a case study. Reg Stud Mar Sci 8:287–296. https://doi.org/10.1016/j.rsma.2016.01.004

Zhang J (2007) Watersheds nutrient loss and eutrophication of the marine recipients: a case study of the Jiaozhou Bay, China. Water Air Soil Poll: Focus 7:583–592. https://doi.org/10.1007/s11267-007-9130-1

Zhang Y, Li F, Zhang Q, Li J, Li Q (2014) Tracing nitrate pollution sources and transformation in surface- and ground-waters using environmental isotopes. Sci Total Environ 490:213–222. https://doi.org/10.1016/j.scitotenv.2014.05.004

Zhang X, Davidson EA, Mauzerall DL, Searchinger TD, Dumas P, Shen Y (2015) Managing nitrogen for sustainable development. Nature 528:51–59. https://doi.org/10.1038/nature15743

Zhang X, Bol R, Rahn C, Xiao G, Meng F, Wu W (2017) Agricultural sustainable intensification improved nitrogen use efficiency and maintained high crop yield during 1980-2014 in Northern China. Sci Total Environ 596(597):61–68. https://doi.org/10.1016/j.scitotenv.2017.04.064

Zhao S, Qiu S, Cao C, Zheng C, Zhou W, He P (2014) Responses of soil properties, microbial community and crop yields to various rates of nitrogen fertilization in a wheat–maize cropping system in north-central China. Agric Ecosyst Environ 194:29–37. https://doi.org/10.1016/j.agee.2014.05.006